REPORT DOCUMENTATION PAGE

Form Approved
OMB No. 0704-0188

1. REPORT DATE *(DD-MM-YYYY)*	**2. REPORT TYPE**	**3. DATES COVERED** *(From - To)*
05-03-2010	Technical Report	

4. TITLE AND SUBTITLE

Green and Ultraviolet Pulse Generation with a Compact, Fiber Laser, Chirped-Pulse Amplification System for Aerosol Fluorescence Measurements

5a. CONTRACT NUMBER

5b. GRANT NUMBER

5c. PROGRAM ELEMENT NUMBER

6. AUTHOR(S)

Janet W. Lou,
Marc Currie,
Vasanthi Sivaprakasam,
Jay Eversole

5d. PROJECT NUMBER
BA09DET001

5e. TASK NUMBER

5f. WORK UNIT NUMBER

7. PERFORMING ORGANIZATION NAME(S) AND ADDRESS(ES)

Optical Sciences Division,
US Navy Research Laboratory
4555 Overlook Ave., S.W., Washington, DC 20375

8. PERFORMING ORGANIZATION REPORT NUMBER

9. SPONSORING / MONITORING AGENCY NAME(S) AND ADDRESS(ES)

Defense Threat Reduction Agency
8725 John J Kingman Road
Fort Belvoir, VA 22060-6201

10. SPONSOR/MONITOR'S ACRONYM(S)

11. SPONSOR/MONITOR'S REPORT NUMBER(S)

12. DISTRIBUTION / AVAILABILITY STATEMENT

Distribution Unlimited/Public Release Unlimited

13. SUPPLEMENTARY NOTES

14. ABSTRACT

We use a compact chirped-pulse amplified system to harmonically generate ultra-short pulses for aerosol fluorescence measurements. The seed laser is a compact, all-normal dispersion, mode-locked Yb-doped fiber laser with a 1050-nm center wavelength operating at 41 MHz. Average powers of more than 1.2 W at 525 nm and 350 mW at 262 nm are generated high-dispersion fiber, amplified by a high-power, large-mode area fiber amplifier, and recompressed using a chirped volume holographic Bragg grating. The resulting high-peak-power pules allow for highly efficient harmonic generation. We also demonstrate, for the first time to our knowledge, the use of a mode-locked ultra-violet source to excite individual biological particles and other collaboration particles in an inlet air flow as they pass through an optical chamber. The repetition rate is ideal for bio-fluorescence measurements as it allows faster sampling rates as well as the higher peak powers as compared to previously demonstrated Q-switched systems while maintaining a pulse period that is longer than the fluorescence recovery time. Thus, the fluorescence excitation can be considered to be quasicontinuous and required no external synchronization and triggering.

15. SUBJECT TERMS

Fiber laser, mode-locked lasers, nonlinear optical devices, harmonic generation, ultrafast spectroscopy, aerosol detection, laser-induced fluorescence

16. SECURITY CLASSIFICATION OF:			**17. LIMITATION OF ABSTRACT**	**18. NUMBER OF PAGES**	**19a. NAME OF RESPONSIBLE PERSON**
Unclassified					Bryan Horner
a. REPORT	**b. ABSTRACT**	**c. THIS PAGE**		6	**19b. TELEPHONE NUMBER** *(include area code)*
					7037673379

Standard Form 298 (Rev. 8-98)
Prescribed by ANSI Std. Z39.18

Green and Ultraviolet Pulse Generation with a Compact, Fiber Laser, Chirped-Pulse Amplification System for Aerosol Fluorescence Measurements

Janet W. Lou, Marc Currie, Vasanthi Sivaprakasam, Jay D. Eversole

Abstract— **We use a compact chirped-pulse amplified system to harmonically generate ultra-short pulses for aerosol fluorescence measurements. The seed laser is a compact, all-normal dispersion, mode-locked Yb-doped fiber laser with a 1050-nm center wavelength operating at 41 MHz. Average powers of more than 1.2 W at 525 nm and 350 mW at 262 nm are generated with <500-fs pulse durations. The pulses are time-stretched with high-dispersion fiber, amplified by a high-power, large-mode-area fiber amplifier, and recompressed using a chirped volume holographic Bragg grating. The resulting high-peak-power pulses allow for highly efficient harmonic generation.**

We also demonstrate, for the first time to our knowledge, the use of a mode-locked ultra-violet source to excite individual biological particles and other calibration particles in an inlet air flow as they pass through an optical chamber. The repetition rate is ideal for bio-fluorescence measurements as it allows faster sampling rates as well as the higher peak powers as compared to previously demonstrated Q-switched systems while maintaining a pulse period that is longer than the fluorescence recovery time. Thus, the fluorescence excitation can be considered to be quasi-continuous and requires no external synchronization and triggering.

***Index Terms*— Fiber lasers, Mode-locked lasers, Nonlinear optical devices, Harmonic generation, Ultrafast spectroscopy, Aerosol detection, Laser-induced fluorescence**

I. Introduction

THE generation of green and ultra-violet wavelength, mode-locked pulses are of great interest for fluorescence measurements of biological media [1], micro-machining, and many other applications that require either high-peak power or quasi-continuous ultra-violet lasers. Bio-threat detection sensors developed recently have used laser induced fluorescence measurement to provide an initial rapid alert, or trigger, to the presence of biological aerosol particles. Methods to reduce the size, power, and cost of such systems are widely pursued. Mode-locked lasers are better suited for bio-fluorescence measurements as compared to previously demonstrated Q-switched systems because mode-locked lasers can operate at higher repetition rates and with a pulse period longer than the fluorescence recovery time, they allow for a faster sampling rate. Additionally, no electronic triggering is required since the system operates in a quasi-continuous mode. Passively mode-locked fiber laser systems that generate short pulses are generally compact and portable. The high peak powers associated with short pulses also make these sources attractive for applications requiring multi-photon processes and/or efficient harmonic generation. In general, it is difficult to amplify short optical pulses without detrimental nonlinear effects. We overcome this limitation by building a band-limited Yb-doped fiber laser with no dispersion compensation similar in design to Ref. 2, as the master oscillator (λ_c = 1050 nm) and use this laser in a chirped-pulse-amplification (CPA) setup to achieve >220-kW peak power output pulses. Frequency-doubling to a wavelength of 525 nm results in ~1.2-W average power and further doubling to a wavelength of 262 nm results in >350-mW average power. In Section III, we will discuss the laser system configuration, followed by our experimental results in Section IV. Then in Section V, we demonstrate the application of mode-locked ultra-violet pulses for particle fluorescence excitation.

Manuscript received April XX. 2010. This work was supported by the Office of Naval Research and the Defense Threat Reduction Agency.

J. W. Lou is with the Mission Systems Division, Global Defense Technology & Systems, Inc., 2200 Defense Highway, Suite 405, Crofton, MD 21114 USA (phone: 202-404-5474; fax: 202-404-8645; e-mail: janet.lou.ctr@nrl.navy.mil).

M. Currie, V. Sivaprakasam, and J. D. Eversole are with the Optical Sciences Division, U.S. Naval Research Laboratory, 4555 Overlook Ave., S. W., Washington, DC 20375 USA.

II. Background

Harmonic frequency generation is a well-known technique for creating continuous-wave as well as pulsed light in the green and ultra-violet wavelengths. However, quadrupling of mode-locked pulses has been rare [3]. Recently, some commercial systems have become available, but their pulse widths are relatively long and their pulse energies are relatively low [4]. Our previously demonstrated fiber laser and CPA system for harmonic generation operated at a much lower repetition rate and hence, lower average power [5]. By operating at a higher repetition rate, we maintain the same pulse energy in the harmonic generation crystals, and achieve higher average powers. In this paper, we report on a system with improved conversion efficiencies and higher output powers. Additionally, we have implemented a chirped volume holographic Bragg grating compressor as in Ref. 6. This

significantly reduces the size and complexity of the pulse compressor as compared to the conventional Treacy compressor [7] as well as increases the power handling capability.

We have recently demonstrated the application of a mode-locked green laser to two-photon fluorescence cross-section studies of bio-aerosols [8]. To our knowledge, there has not been a demonstration of the use of mode-locked ultra-violet pulses for single-photon fluorescence measurements. We will present fluorescence measurement results for both dye-doped polystyrene latex (PSL) particles and biological particles.

III. Laser Configuration

To achieve the high peak powers in the fundamental wavelength pulses that are necessary for efficient conversion and ultimately, significant power levels in the ultra-violet wavelength, we implement a fiber CPA technique. In order to create a compact, lightweight, and fieldable system, we develop a normal-dispersion Yb-doped fiber laser, which is followed by a single-mode Yb-doped fiber preamplifier, high-dispersion fiber for temporal stretching of the pulses, a multi-stage, large-mode-area, Yb-doped fiber power amplifier, and finally a chirped volume holographic Bragg grating to recompress the pulses. Frequency conversion to a wavelength of 525 nm is achieved with a lithium triborate (LBO) crystal and further conversion to a wavelength of 262 nm is achieved with a beta barium borate (BBO) crystal. A schematic diagram of the overall system is illustrated in Fig. 1.

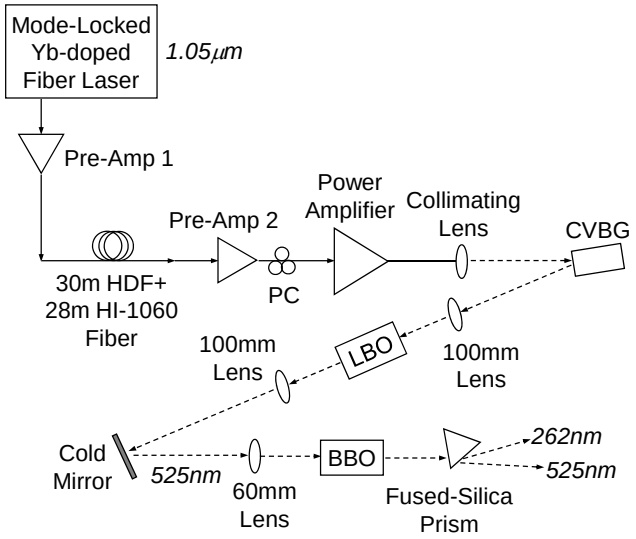

Fig. 1: Schematic diagram of system. The solid line represents the optical path through optical fibers and the dashed line represents the beam path through free space. CPA = chirped pulse amplification, SHG = second harmonic generation, Yb = ytterbium, HDF = high-dispersion fiber, CVBG = chirped volume Bragg grating, PC = polarization controller, LBO = lithium triborate crystal, and BBO = beta barium borate crystal.

A detailed schematic diagram of the laser configuration is shown in Fig. 2(c). Because the laser does not require dispersion compensation, it can be made very compact and robust by using all fiber components. The laser gain media is a 3-m length of single mode Yb-doped fiber with a 4.4-μm core size (INO Yb118). Passive mode-locking is achieved by nonlinear polarization rotation. Once the static polarization is properly set, the laser is self mode-locking with ~135-mW of power at the 976-nm pump wavelength. The 10-nm intra-cavity spectral filter (CVI) not only aids in mode-locking, but also constrains the required bandwidth of the compressor. Additionally, by adjusting the angle of incidence to the filter, the fundamental wavelength can be tuned. The average output power of the laser is ~3.5 mW, after the 1.66-dB loss of the output single-stage optical isolator (General Photonics). The isolator is necessary to stabilize the laser, as back-reflections can disturb the mode-locking. The output pulse is chirped with an autocorrelation width of ~5 ps and a spectral full-width-at-half-maximum (FWHM) width of 8.3 nm, centered at 1050 nm. A typical autocorrelation and spectrum are shown in Figs. 2(a) and 2(b), respectively.

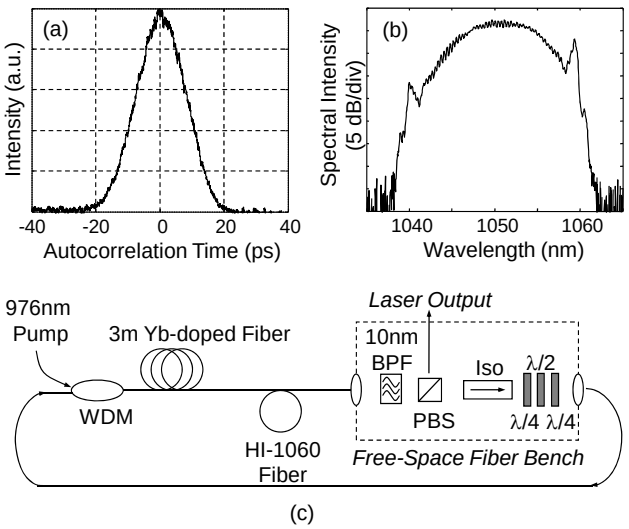

Fig. 2: Laser configuration (c) and typical output pulse (a) autocorrelation and (b) spectrum. WDM = wavelength-division-multiplexer, Yb = ytterbium, PBS = polarization beam splitter, BPF = band-pass filter, and Iso = isolator.

The chirped pulse amplification segment of the setup is illustrated in Fig. 3, where insets show the temporal pulse shape and spectrum. The stretched pulse, as detected by a Thor Labs D400FC InGaAs detector and Agilent Infiniium 86109A optical detector plug-in module, is also shown in Fig. 3. First the laser output is amplified using an Yb-doped fiber preamplifier (Pre-Amp 1) with ~1.1 m of gain fiber that has a core size of 7 μm (INO Yb708). The gain fiber is end-pumped with 550 mW of 976-nm pump in a counter-propagating configuration. The output power is ~55 mW. Stretching the pulse to ~125-ps duration is achieved with the combination of a 30-m length of Corning high-dispersion fiber (D=-100ps/nm/km) and ~28-m length of Corning HI-1060 fiber (D~-35ps/nm/km). The loss of the fiber stretcher is almost 6 dB because the high-dispersion fiber is designed for a wavelength of 980 nm. A single-mode, large-mode-area, Yb-doped fiber (Liekki Yb1200-10/125DC) preamplifier (Pre-Amp 2) is used to amplify the stretched pulse to ~155-mW average power. The 0.85-m length gain fiber has a core size of 9.7 μm and is co-propagating, end-pumped with 500 mW of 976-nm pump. This is then followed by a double-clad fiber amplifier with a 1.65-m length, 20-μm core gain fiber (Liekki

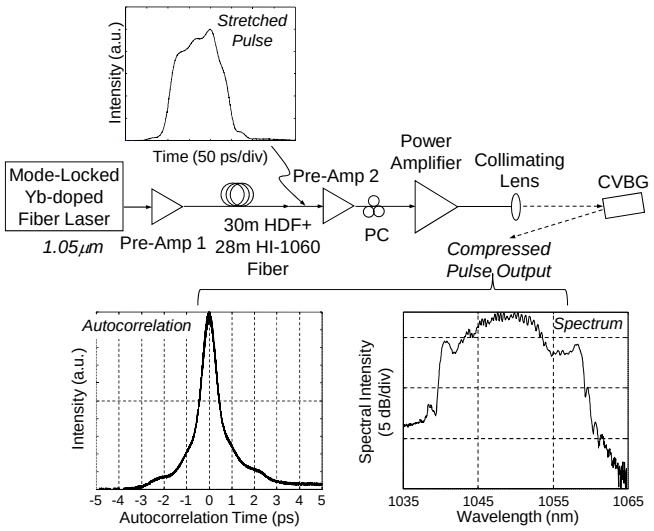

Fig. 3: Chirped-pulse amplification setup. The stretched pulse is detected by a fast photodetector and measured with an oscilloscope. The compressed pulse is measured with an intensity autocorrelator and the spectrum is characterized with an optical spectrum analyzer. Yb = ytterbium, HDF = high-dispersion fiber, CVBG = chirped volume Bragg grating, and PC = polarization controller.

Yb1200-20/125DC). This amplifier has four 976-nm wavelength pump laser diodes (Alfalight) that each have a maximum output power of 4 W, which are coupled via a multimode coupler (SIFAM) and counter-propagating to the signal. The output power of the amplifier versus the total pump power is plotted in Fig. 4, and the maximum output

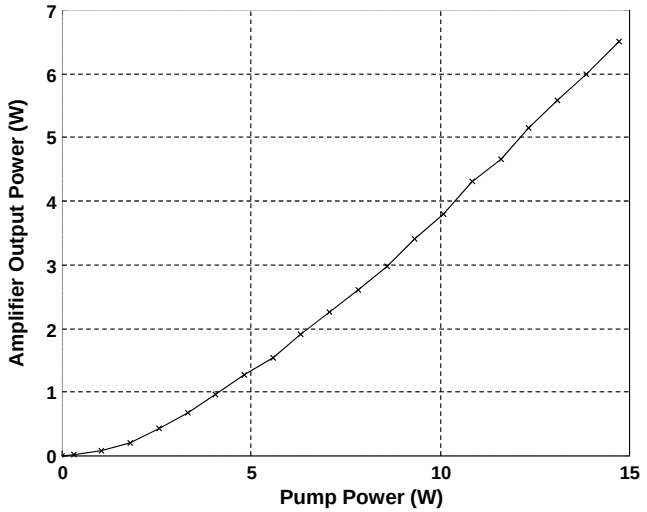

Fig. 4: Power amplifier performance. The plot shows the measured output power versus the input pump power. The input pump power is calculated based on the drive current and efficiency of the laser diode.

power is ~6.5 W for ~15 W of pump power, indicating over 43% pump efficiency. The power amplifier output is collimated with a 25-mm lens, anti-reflection coated for the wavelength range of 650 to 1050 nm. Finally, the pulses are recompressed using a chirped volume holographic Bragg grating (Optigrate) with a reflection bandwidth of 20 nm. The characteristic spectral reflection response function is illustrated in Fig. 5. The reflected power is ~69% of the total incident power, as shown in Fig. 6, and we achieve a maximum output of ~4.5 W. The size of the grating is

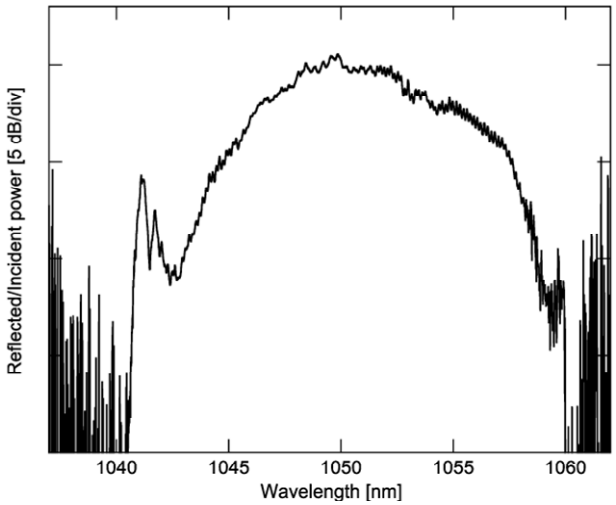

Fig. 5: Characteristic spectral reflection response of the chirped volume holographic Bragg grating.

4x8x25mm and both end facets are anti-reflection coated. The recompressed pulse, shown in Fig. 3, has an autocorrelation width of ~670 fs with some pedestals, which are likely due to higher order dispersion effects. The expected transform-limited pulse width for a normal-dispersion laser with this spectral width is ~454 fs [2].

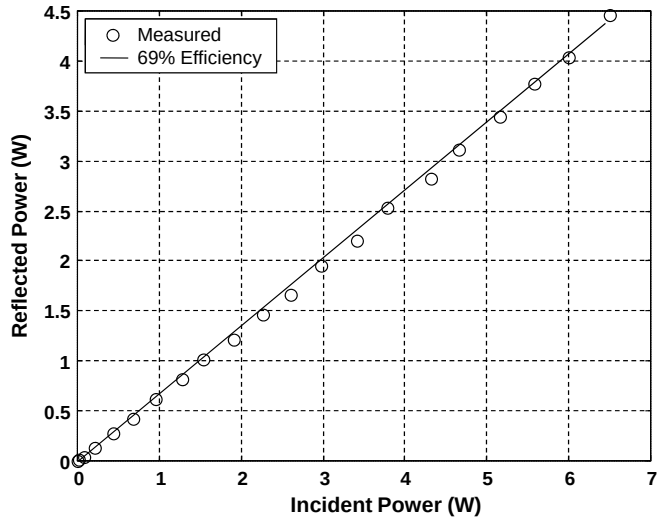

Fig. 6: Reflected power performance of the chirped volume holographic Bragg grating. The reflected power is ~69% of the incident power.

The harmonic generation segments comprise the final stages of the system. The crystals and lenses are all anti-reflection coated for the fundamental and/or the second harmonic frequencies. The polarization controller, located between Pre-Amp 2 and the power amplifier, is used to align the amplifier output polarization to the axis of the crystals. A 100-mm lens is used to focus into the 5x5x20-mm length LBO crystal (Coherent) and a 100-mm lens is used to collimate the output. The spot size inside the crystal is approximated by using a knife-edge measurement technique in free-space at the approximate center location of the crystal. The beam is measured to be ~64-μm FWHM (~109-μm "$1/e^2$" width). Estimating the crystal refractive index as 1.56, a calculated 45-

mm confocal parameter implies a fairly uniform intensity within the LBO crystal. A cold mirror is used to separate the 1050-nm and 525-nm wavelengths, and the latter is focused into the 4x4x6-mm length BBO crystal (Optical Planz) with a 60-mm lens for 262-nm wavelength generation. Again, using the knife-edge measurement technique, the spot size in free-space is ~75-μm FWHM (~127μm "$1/e^2$" width). And again using a refractive index of 1.56, the calculated 120-mm confocal parameter is much longer than the crystal, thereby insuring a uniform intensity beam inside the crystal. The output of the BBO crystal is followed by a fused silica prism for separating the green and ultra-violet wavelengths.

IV. Results

Figure 7 illustrates the second harmonic generation results. Figure 7(a) represents the measured power conversion from 1050-nm to 525-nm wavelength. Figure 7(b) shows the calculated conversion efficiency as a function of the input power. The efficiency improves with increased power until an input power level of ~3 W when it reaches the maximum conversion efficiency of ~30%. No saturation in output power is observed up to our maximum average input power of 4.5 W, resulting in an output power of 1.25 W and a pulse energy of ~30.5 nJ. The spectrum of this second harmonic pulse is shown in Fig. 8, and the FWHM width is ~0.8 nm. This is narrower than expected and is probably due to a combination of effects including the chirp on the input pulse as well as the LBO acceptance angle and phase matching characteristics.

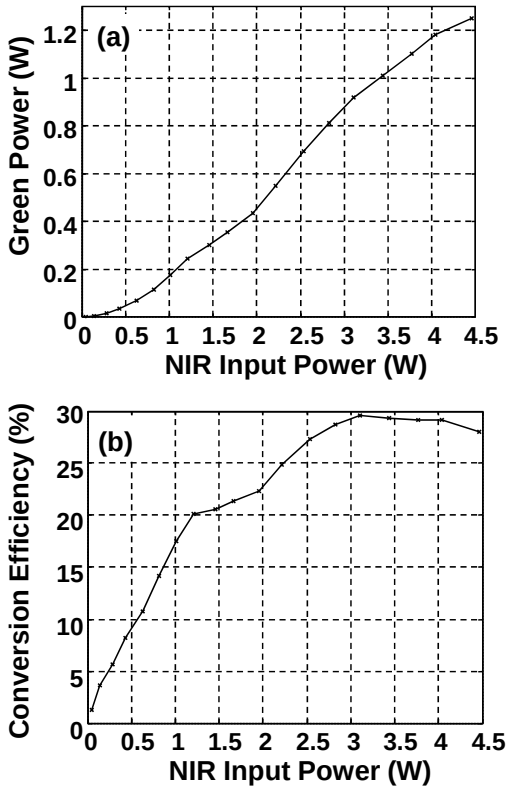

Fig. 7: Performance of the second harmonic generation process. (a) Measured power conversion from 1050 nm to 525 nm wavelengths, (b) Calculated conversion efficiency versus input power.

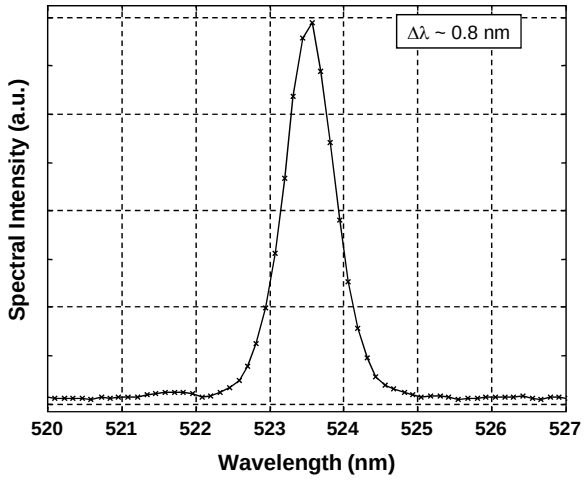

Fig. 8: Spectrum of the 525-nm pulses. The FWHM width is ~0.8 nm.

Figure 9 illustrates the measured performance of the conversion from 525 nm to 262 nm (fourth harmonic of the fundamental wavelength). Figures 9(a) and 9(b) represent the power conversion from the 525 nm to the 262 nm wavelength, and the calculated conversion efficiencies, respectively. In this case, the peak conversion efficiency is ~28%. Again, no power saturation effects are observed and a maximum average output power ~350 mW is achieved, providing a maximum pulse energy of ~8.5 nJ. The spectrum of this fourth harmonic is shown in Fig. 10, and the FWHM width is ~0.6 nm.

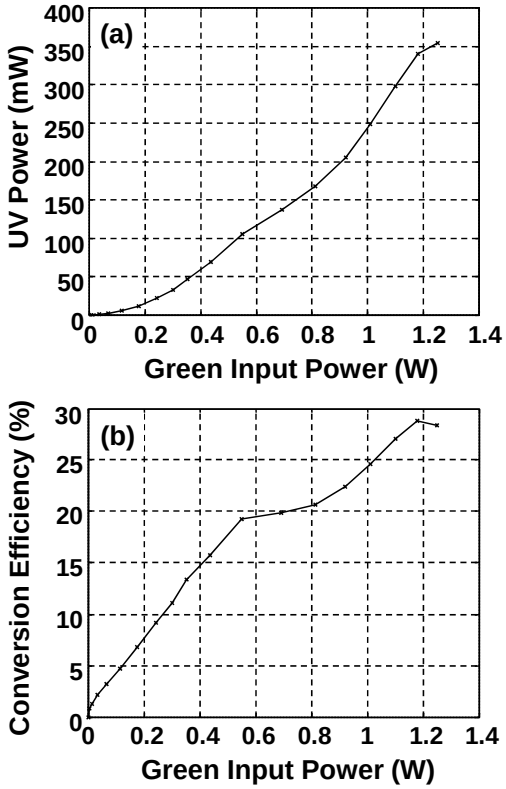

Fig. 9: Performance of the uv generation process. (a) Measured power conversion from 524 nm to 262 nm wavelengths, (b) Calculated conversion efficiency versus input power.

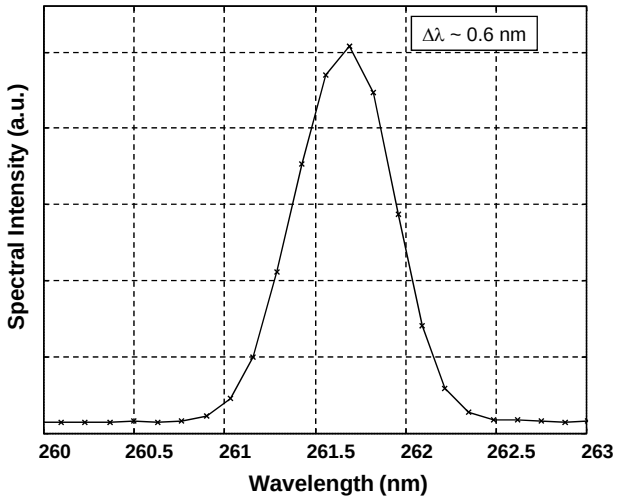

Fig. 10: Spectrum of the 262-nm pulses. The FWHM width is ~0.6 nm.

Because of phase matching and acceptance angle requirements, the harmonic generation processes leads to an elliptically shaped output beam. Figures 11(a) and 11(b) shows the beam intensity profiles of the green and ultra-violet output beams, respectively. The minor to major axis ratio is ~0.6 in both cases.

Finally, another parameter of interest in these systems is the electrical-optical conversion efficiency. Based on the DC voltage and current of all the laser diode drivers and thermo-electric coolers, we calculate the electrical to ultra-violet (optical) conversion efficiency to be ~0.4% and ~1.5% for the conversion to the green wavelength.

Note that the multimode coupler used for the power amplifier pumps has 6 possible inputs. Since we are currently using just 4 pumps, there are still 2 remaining, unused, ports. Thus, the system could achieve even higher output powers by simply adding pumps to those ports.

V. Fluorescence Excitation

We conduct several proof-of-principle experiments to show that mode-locked ultra-violet pulses can be used effectively for fluorescence excitation and particle detection. The Aerosol Interrogation Module breadboard used for our mode-locked laser studies has been described previously elsewhere [9]. The aerosol particles are pumped through a 700-µm aerosol nozzle into the focal volume of the aerosol chamber where the individual micron-sized particles are interrogated. The scattered and fluorescence light are collected by an elliptical reflector and sampled in several broad bandwidth detection bands. The ultra-violet beam is focused to form a 730-µm by 350-µm beam in the focal volume of the elliptical collection mirror. The particles flow at a median velocity of roughly 4.3 m/s, which translates to a transit time through the beam of 83 µs. The entire signal is integrated by setting the electronic gate width for the integrator to be 100 µs.

The fluorescence and elastic scatter are measured from a number of calibration PSL particles and biological agent simulant particles. The fluorescence signal and elastic scatter

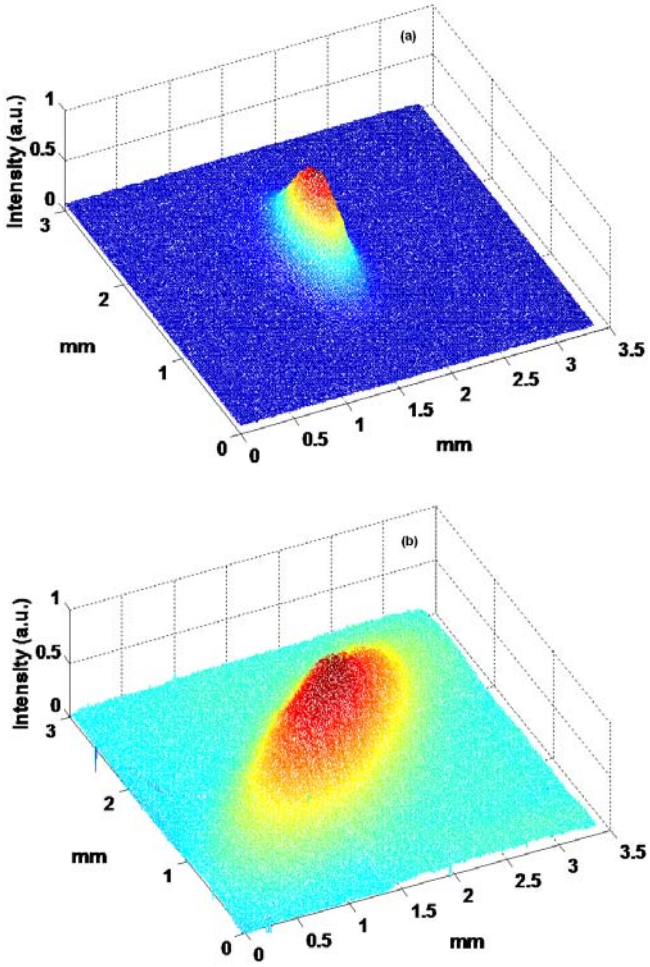

Fig. 11: Beam intensity profile of the (a) 525-nm wavelength pulses, and (b) 262-nm wavelength pulses.

signal as a 10-µm NaCl particle doped with tryptophan transits through the laser beam is shown in Fig. 12. The quasi-continuous nature of this excitation is evident in these plots. The particle is continuously excited by different pulses as it traverses the beam. The fluorescence emission from the

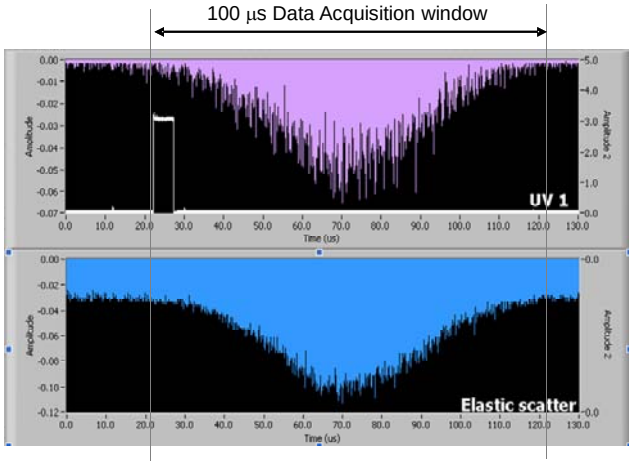

Fig. 12: The fluorescence and elastic scatter signal as a 10-µm NaCl particle doped with tryptophan is traversing through the beam.

tryptophan in the 300 to 340-nm band is shown in the top trace and the elastic scatter signal is shown in the bottom trace. The DC background level seen in the elastic scatter signal is due to the stray scattered light from the aerosol chamber. The signals are integrated, corrected for the various instrument responses, and expressed as number of photons emitted by the particle.

The fluorescence of a size series of green dye-doped PSL spheres ranging in size from 2 to 5 μm is plotted in Fig. 13.

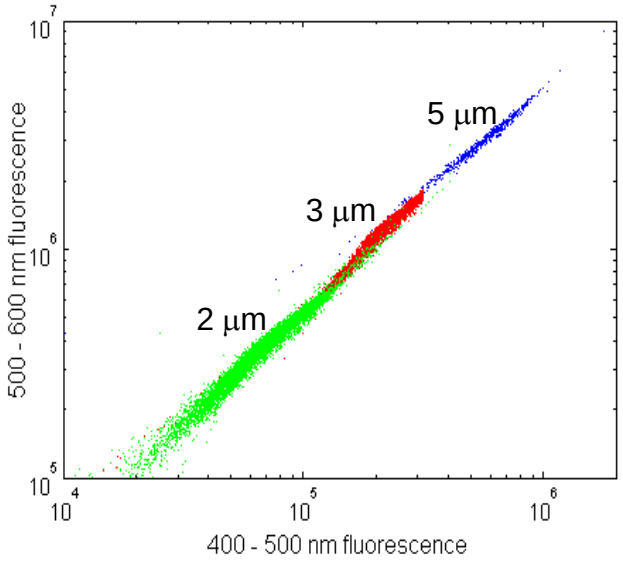

Fig. 13: The fluorescence in the 400 – 500 nm band versus in the 500 – 600 nm band for 2, 3, and 5 μm green dye-doped PSL particles.

Roughly 10,000 particles are sampled for each particle size. The fluorescence emission measured in the 400 to 500-nm band is plotted versus the fluorescence emitted in the 500 to 600-nm band. As expected, the fluorescence signal scales with particle size and the distribution of the particles is much tighter for the bigger size particles. In fact, the fluorescence signal shows an approximately cubic dependence on the particle size as one would expect from homogenous particles.

The fluorescence measured from the bio-warfare agent simulants Bacillus Globigii (BG) and ovalbumin is shown in Fig. 14. BG is a simulant for anthrax spores and ovalbumin is a common simulant for biological toxins. The particles are generated using a Sono-tek generator and the mass median size for BG and ovalbumin are 4.7 μm and 5.8 μm, respectively, with a FWHM of less than 2 μm. The fluorescence in the 300 to 340-nm band is plotted versus the 360 to 400-nm fluorescence band. These fluorescent bands are the prominent protein signature bands for biological materials. As one can observe from the fluorescence emission from the bacterial spores (Fig. 14), the BG signature is well separated from that of ovalbumin. The fluorescence signature shows wider distribution due to the wider range of particle sizes in the sample. These preliminary measurements on bioaerosols from mode-locked ultra-violet excitation are encouraging.

VI. Conclusion

We demonstrate ultra-short pulsed harmonic generation to 525-nm and 262-nm wavelengths starting with a 41-MHz

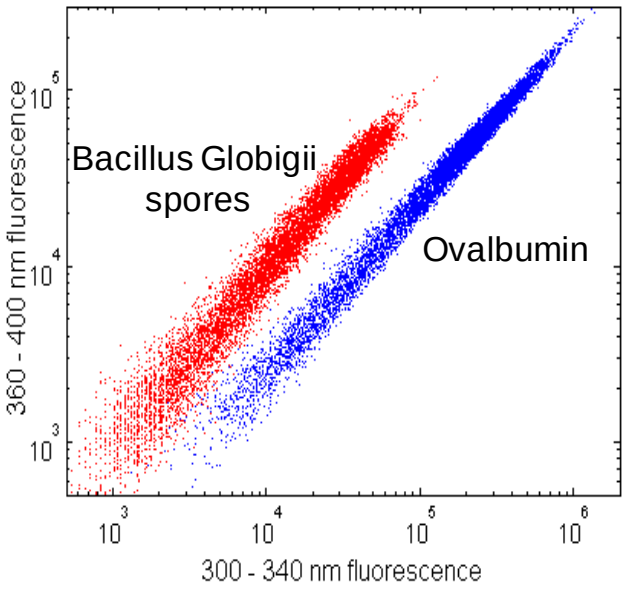

Fig. 14: The fluorescence of 2 simulant samples: BG and ovalbumin.

mode-locked, all-normal-dispersion, Yb-doped fiber laser with a center wavelength of 1050 nm. Nonlinear effects during amplification are reduced through the implementation of chirped-pulse amplification. Frequency doubling results in average powers of greater than 1.2 W (30.5 nJ/pulse) for the 525-nm wavelength and 350 mW (8.5 nJ/pulse) for the 262-nm wavelength with <500-fs pulse durations. We also demonstrate that mode-locked ultra-violet pulses generated by a fiber laser are viable sources for fluorescence excitation of biological particles.

References

[1] V. Sivaprakasam, J. Czege, J. Lou, M. Currie, and J. D. Eversole, "*Fluorescence from biological aerosol particles using mode-locked laser pulses: one and two photon excitation*", Pittsburgh Conference, Orlando, FL, Paper 2020-8, 2010.

[2] J. W. Lou, M. Currie, and F. K. Fatemi, "*Experimental Measurements of Solitary Pulse Characteristics from an All-Normal-Dispersion Yb-doped Fiber Laser*", Opt. Express, 15, 8, pp.4960-4965, 2007, http://www.opticsinfobase.org/abstract.cfm?URI=oe-15-8-4960.

[3] J. C. Garcia, A. K. Newman, J. M. Liu, and M. C. Lee, "*Cw mode-locked deep UV pulses at an average power of 1.8 W*", J. Opt. A: Pure Appl. Opt., 2, pp. L41-L43, 2000.

[4] http://www.fianium.com/uvpower.htm.

[5] J. W. Lou and M. Currie, "*Green and Ultraviolet Pulse Generation Using a Low-Repetition-Rate Mode-Locked Yb-Doped Fiber Laser*", Conf. on Lasers and Electro-Optics, Baltimore, MD, JWA38, 2007.

[6] G. Chang, C.-H. Liu, K.-H. Liao, V. Smirnov, L. Glebov, and A. Galvanauskas, "*50-W Chirped-Volume-Bragg-Grating Based Fiber CPA at 1055-nm*", Conf. on Lasers and Electro-Optics, Baltimore, MD, CMEE4, 2007.

[7] E. B. Treacy, "*Optical pulse compression with diffraction gratings*", IEEE J. Quantum Electron., QE-5, 9, pp. 454-458, 1969.

[8] V. Sivaprakasam, J. W. Lou, M. Currie, and J. D. Eversole, "*Two-photon excited fluorescence from bioaerosol particles*", to be submitted 2010.

[9] V. Sivaprakasam, T. Pletcher, J. E. Tucker, A. L. Huston, J. McGinn, D. Keller and J. D. Eversole, "*Classification and Selective Collection of Individual Aerosol Particles Using Laser-Induced Fluorescence*", Appl. Opt., 48, 4, pp.B126-B136, 2009.